Non-equilibrium entropy and dynamics in a system with long-range interactions

IOP Publishing Journal of Physics A: Mathematical and Theoretical
J. Phys. A: Math. Theor. **49** (2016) 185002 (15pp) doi:10.1088/1751-8113/49/18/185002

Non-equilibrium entropy and dynamics in a system with long-range interactions

T M Rocha Filho

Instituto de Física and International Center for Condensed Matter Physics Universidade de Brasília, CP: 04455, 70919-970—Brasília, Brazil

Received 12 January 2015, revised 7 December 2015
Accepted for publication 8 January 2016
Published 29 March 2016

Abstract

We extend the core-halo approach of Levin *et al* (2014 *Phys. Rep.* **535**, 1) for the violent relaxation of long-range interacting system with a waterbag initial condition, in the case of a widely studied Hamiltonian mean field model. The Gibbs entropy maximization principle is considered with the constraints of energy conservation and of coarse-grained Casimir invariants of the Vlasov equation. The core-halo distribution function depends only on the one-particle mean-field energy, as is expected from the Jeans theorem, and depends on a set of parameters which in our approach is completely determined without having to solve an envelope equation for the contour of the initial state, as required in the original approach. We also show that a different ansatz can be used for the core-halo distribution with similar results. This work also reveals a link between a parametric resonance causing the non-equilibrium phase transition in the model, a dynamical property, and a discontinuity of the (non-equilibrium) entropy of the system.

Keywords: long-range interactions, violent relaxation, Hamiltonian mean field model

(Some figures may appear in colour only in the online journal)

1. Introduction

If the pair-interaction potential of a many-body system $V(\mathbf{r}-\mathbf{r}')$ decays at long distances $r=|\mathbf{r}-\mathbf{r}'|$ as $1/r^{\alpha}$ with α smaller than the spatial dimension, then the system is said to be long-range interacting. This includes the relevant cases of gravitational and non-shielded Coulomb interactions. These systems present some unusual behavior when compared to short-range interacting systems, such as negative specific heat in the microcanonical ensemble, non-ergodicity and non-Gaussian quasi-stationary states (QSSs) [1]. Starting from an initial configuration, an isolated many-particle system with long-range interactions evolves

rapidly though a violent relaxation into a QSS which relaxes to equilibrium with a characteristic time diverging with the number of particles N [2, 3], or in some cases oscillates around a QSS [4]. Predicting the outcome of the violent relaxation has been a major problem in astrophysics for at least half a century, and has drawn much attention in plasma physics and related fields. The first attempt at a statistical theory of violent relaxation is due to Lynden-Bell [8] and is based on the Vlasov equation description, valid for short times for the one-particle distribution function [3, 9]. For a system of identical particles with mass m it is given by:

$$\dot{f} = \frac{\partial f}{\partial t} + \frac{\mathbf{p}}{m} \cdot \frac{\partial f}{\partial \mathbf{r}} + \mathbf{F}(\mathbf{r}, t) \cdot \frac{\partial f}{\partial \mathbf{p}} = 0, \tag{1}$$

where $\mathbf{r}$ and $\mathbf{p}$ are the position and momentum vectors respectively, $f \equiv f(\mathbf{r}, \mathbf{p}, t)$ the one-particle distribution function, and the mean-field force at position $\mathbf{r}$ and time t is:

$$\mathbf{F}(\mathbf{r}, t) = -\nabla \overline{V}(\mathbf{r}, t), \ \overline{V}(\mathbf{r}, t) \equiv \int V(\mathbf{r} - \mathbf{r}') f(\mathbf{r}', \mathbf{p}', t)\, d\mathbf{r}' d\mathbf{p}', \tag{2}$$

where $\overline{V}(\mathbf{r}, t)$ is the mean-field potential. The Vlasov equation admits infinitely many Casimir invariants of motion of the form

$$C_s[f] = \int s(f(\mathbf{r}, \mathbf{p}, t))\, d\mathbf{r} d\mathbf{p}, \tag{3}$$

for any function s. Setting $s = -k_B f \ln f$ in equation (3) results in the Boltzmann entropy (with k_B the Boltzmann constant) which is constant as the Vlasov equation is reversible. Assuming a complete mixing of micro-cells of the same f-levels into coarse grained macro-cells, and maximizing the entropy given by the logarithm of the number of possibilities of distributing non-overlapping microcells (f is constant along phase trajectories) into all macro-cells, Lynden-Bell determined the distribution function resulting from a violent relaxation. Although elegant, this approach is only valid as a first approximation, as pointed out by Lynden-Bell himself (see [11] for a review in astrophysics applications). Different tentative improvements were proposed in the literature by Shu [12], Kull, Treumann and Böhringer [13] and Nakamura [14], although none proved to be completely satisfactory [15, 16].

Parametric resonance is known to play a major role in plasmas as an important phenomenon in the long-time evolution of the system, and has been studied in the context of a single wave-particle interaction [17, 18]. Taking into account this mechanism, and using Jeans's theorem which states that in a steady state the distribution function f depends on position and momentum only through constants of motion [10], Levin and collaborators [19–26] proposed that for a waterbag initial distribution of the form

$$f(\mathbf{r}, \mathbf{p}, 0) = \eta\, \Theta(r_0 - |\mathbf{r}|)\Theta(p_0 - |\mathbf{p}|), \tag{4}$$

with η a normalization constant and Θ the Heaviside step function, the final distribution function after violent relaxation assumes a core-halo structure given by:

$$f(\mathbf{r}, \mathbf{p}, t_v) = \eta\, \Theta(e_F - e(\mathbf{r}, \mathbf{p})) + \chi\, \Theta(e(\mathbf{r}, \mathbf{p}) - e_F)\Theta(e_H - e(\mathbf{r}, \mathbf{p})), \tag{5}$$

with $e(\mathbf{r}, \mathbf{p})$ the one-particle energy:

$$e(\mathbf{r}, \mathbf{p}) = \frac{p^2}{2\, m} + \overline{V}(\mathbf{r}), \tag{6}$$

where e_F and e_H are called the Fermi and halo energies, respectively, χ is a constant parameter fixed by the normalization condition and η has the same value as the initial condition f-value in equation (4). A similar type of distribution function was used in [27] in

the study of the free electron laser, by applying the approach of [28] which derives from the original Lynden-Bell theory for violent relaxation.

The characteristic time for violent relaxation t_v is defined as the mean-field relaxation time into a stationary state of the Vlasov dynamics, which is much shorter than the collisional relaxation to thermodynamic equilibrium (see [8] for an estimation of t_v for a self-gravitating system). The first term in the right-hand side of equation (5) corresponds to the core of the distribution and the second term to the halo. The halo is populated by particles expelled by a parametric resonance in wave–particle interactions which injects particles at higher energies. The halo energy e_H in equation (5) corresponds to the highest energy attained by resonant particles, which in the original approach is determined by solving an envelope equation for the evolution of the contour of the initial waterbag distribution [26]. This approach was applied with reasonable success for one- and two-dimensional self-gravitating systems, non-neutral plasmas and the Hamiltonian mean field (HMF) model (see [19] and references therein).

Despite its success, the core-halo approach still requires us to determine e_H by solving a dynamical equation (the envelope equation), which is not always a simple task, or by determining the halo energy from a molecular dynamics (MD) simulation, in contrast to Lynden-Bell's approach that only presupposes a good mixing of phase elements (values of the distribution function f). One of the goals of this paper is to show that by using an entropy maximization principle, no dynamical equation(s) has(have) to be explicitly solved for. We illustrate our approach by applying it to the HMF model that has played an important role as a paradigmatic model, solvable at equilibrium and retaining some important features of the dynamics of long-range interacting systems, yet being simple enough to allow large-scale MD simulations with numeric effort scaling with the number of particles N instead of N^2 as for most systems of interest [2, 30–35].

The structure of the paper is as follows. In the next section we present the HMF model and study its non-equilibrium phase diagram for an initial waterbag state by applying to it the core-halo approach as described by Pakter and Levin [22]. In section 3 we introduce the variational approach as an alternative method to determine the remaining parameter e_H in the core-halo distribution as given in equation (5), and also discuss the possibility of using a different ansatz for the core-halo configuration. We close the paper with some concluding remarks in section 4.

2. The Hamiltonian mean field model

The Hamiltonian for the HMF model is given by [35]:

$$H = \sum_{i=1}^{N} \frac{p_i^2}{2} + \frac{1}{N} \sum_{i<j=1}^{N} [1 - \cos(\theta_i - \theta_j)], \tag{7}$$

with θ_i the position angle of particle i and p_i its conjugate momentum. At equilibrium, it exhibits a phase transition from a paramagnetic (homogeneous) phase at higher energies to a ferromagnetic (non-homogeneous) phase at lower energies. For non-equilibrium states, a similar phase transition is also observed but with a more intricate structure with a first- or second-order transition and phase reentrances depending on the initial energy and magnetization, which do not coincide with predictions from Lynden-Bell theory [36–39]. Using large-scale molecular dynamics simulations and numerical solutions of the Vlasov equation [42, 44], the author and collaborators have shown that this phase structure is in fact much more complex than previously described, with cascades of phase reentrances near the

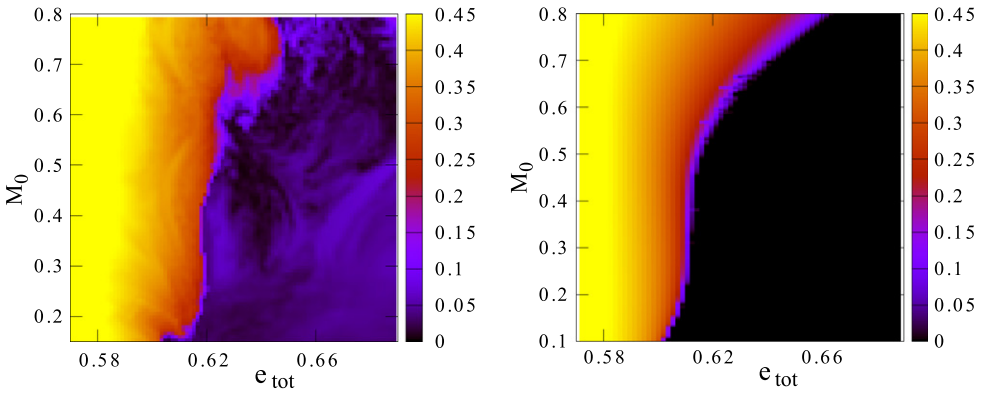

Figure 1. Left panel: final magnetizations for the HMF model as a function of initial magnetization M_0 and total energy per particle e_{tot} from numeric solutions of the Vlasov equation. The grid in (M_0, e_{tot}) space is formed by 100 × 100 simulations with $t_f = 1000.0$ and a numerical grid of 1024 × 1024 points. The final magnetization was obtained by averaging from $t = 800.0$ to $t = 1000.0$. Right panel: predictions from Lynden-Bell theory.

discontinuous phase transition [43]. Non-equilibrium phase transitions in this model can be studied by solving the Hamiltonian equations of motion by using a numerical integrator or solving the corresponding Vlasov equation. For the latter case, a semi-Lagrangian second-order method in time with a fixed time step is used (see [42] for details), and integrated for a sufficiently long time such that after the initial waterbag state the system has settled down in a QSS up to some long-lasting oscillations [43]. Figure 1 shows in greater detail than previous results the non-equilibrium phase diagram of the HMF model from the numeric solution of the Vlasov equation and from Lynden-Bell theory [29]. Although predicting within some accuracy the transition line in the (M, e)-plane, it misses the finer details, such as phase reentrances and even the nature of the phase transition (discontinuous instead of continuous in some energy range) [43].

The total energy of the system can also be written as

$$H = N[K + 1 - M_x^2 - M_y^2], \tag{8}$$

where K is the kinetic energy per particle $K = (1/N)\sum_i p_i^2/2$ and M_x and M_y the magnetization components in the x and y directions, respectively:

$$M_x = \frac{1}{N}\sum_{i=1}^{N}\cos(\theta_i), \tag{9}$$

$$M_y = \frac{1}{N}\sum_{i=1}^{N}\sin(\theta_i). \tag{10}$$

The Fermi energy e_F and the level of the halo χ are determined from the normalization condition:

$$\int \mathrm{d}p\ \mathrm{d}\theta f(p, \theta) = 1, \tag{11}$$

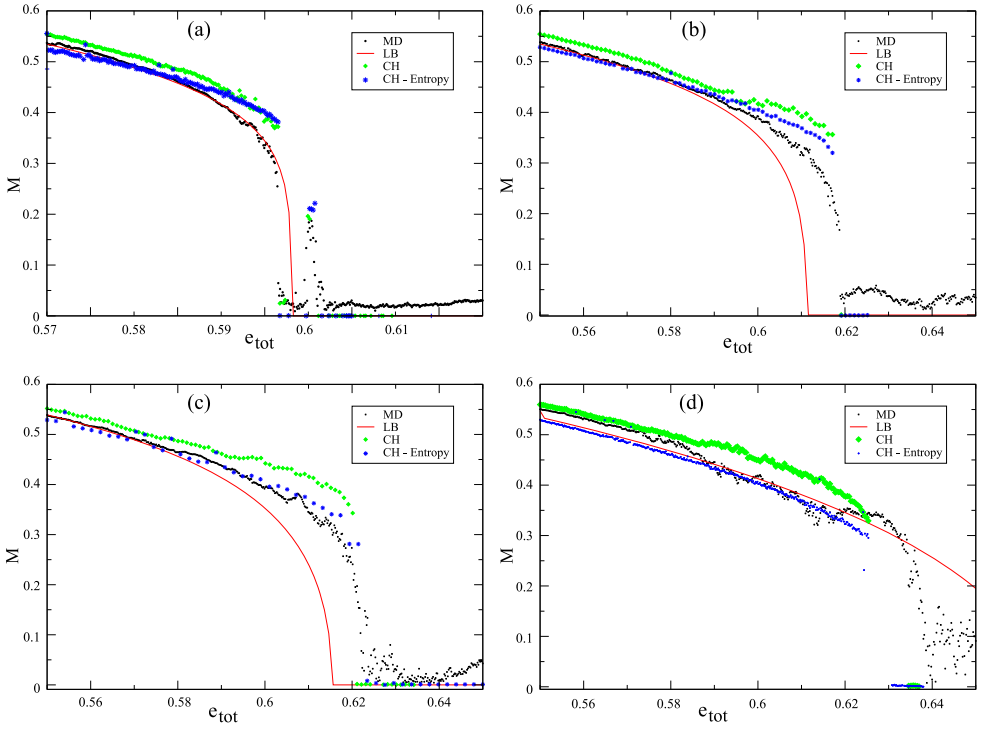

Figure 2. Final magnetizations for the HMF model as a function of total energy per particle e_{tot} from molecular dynamics (MD) simulations from $N = 2\,000\,000$ particles and total simulation time $t_f = 10\,000$, from Lynden-Bell (LB), core-halo theory (CH) with halo energy e_h obtained from the largest one-particle energy in the MD simulation, and CH theory with e_h with entropy maximization procedure (CH-Entropy). Initial magnetizations are: (a) $M_0 = 0.15$, (b) $M_0 = 0.3$, (c) $M_0 = 0.5$ and (d) $M_0 = 0.8$.

and energy conservation

$$\int \mathrm{d}p\ \mathrm{d}\theta \left[\frac{p^2}{2} + \frac{1}{2}\,\overline{V}\,(\theta)\right] f\,(p,\,\theta) = e_{\mathrm{tot}}, \tag{12}$$

where e_{tot} is the total energy divided by the particle number N. The final magnetization is determined self-consistently as:

$$M = \int \mathrm{d}p\ \mathrm{d}\theta \cos(\theta) f\,(p,\,\theta), \tag{13}$$

after setting the origin of the angles such that $M_y = 0$ and $M_x = M \geqslant 0$. The corresponding expression for the mean field potential is:

$$\overline{V}\,(\theta) = \int \mathrm{d}p' \mathrm{d}\theta' [1 - \cos(\theta - \theta')] f\,(p',\,\theta') = 1 - M\cos(\theta). \tag{14}$$

Figure 2 shows, for a few different values of the initial magnetizations M_0, a comparison of MD simulations, Lynden-Bell (LB) theory and the core-halo (CH) approach with the distribution in equation (5) and e_H determined from the highest one-particle energy from the same MD simulations. MD simulations were performed using a graphics processing unit parallel implementation of a fourth-order symplectic algorithm [41, 42]. We note that due to

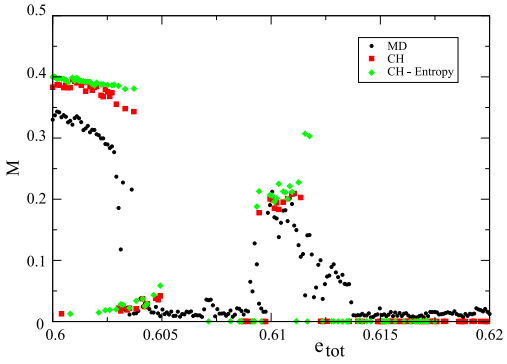

Figure 3. Zoom over figure 2(a) with a close look at the phase reentrance details for initial magnetization $M_0 = 0.15$ and comparing MD simulations, CH and CH-Entropy as in figure 2.

the periodic boundary conditions the envelope equation is harder to solve in the present case [22]. The CH approach predicts accurately the critical energy for the ferromagnetic–paramagnetic transition in all cases but with quantitative discrepancies for the magnetization. In the paramagnetic phase, the average magnetization from MD simulations does not vanish as a consequence of very-long lasting oscillations of the spatial distribution around a QSS, the latter having a vanishing magnetization. Is is important to note that such oscillations can last for a very long time or even forever [4] and thus cannot be described by a static distribution function. Nevertheless the vanishing average of each component of the magnetization is correctly predicted [22, 43]. In figure 2(a) a phase reentrance is clearly visible and its position is accurately predicted by the CH approach. A closer look at the phase reentrance region is given in figure 3. Some deviations from the numerical values of M are due to the fact that the ansatz in equation (5) is too simple and cannot grasp all the details of a more complex distribution function (see figure 7 below).

3. Variational method: entropy maximization

The very long relaxation time to thermodynamic equilibrium of a system with long-range interactions, which diverges with N [2, 3, 46], is a consequence of the existence of the infinitely many Casimir constants of motion of the Vlasov equation (1). Those are usually incompatible with the values of the Boltzmann equilibrium distribution $\mathcal{C}\exp[-\beta e(\mathbf{r}, \mathbf{p})]$, with $\mathcal{C}$ a normalization constant and $e(\mathbf{r}, \mathbf{p})$ given in equation (6). Consequently the system can never attain equilibrium in the limit $N \to \infty$, and eventually settles in a stationary state of the Vlasov equation (or oscillates around it). For finite N, collisional effects (graininess) become important and the system is in a QSS which relaxes very slowly to equilibrium [3]. In [47] it was shown that the stability conditions for a homogeneous QSSs of the HMF model as obtained in [30] are equivalent to maximizing the Gibbs entropy subject to the constraints of energy conservation, normalization and all the analytic Casimirs (i.e. with an analytic function s in equation (3)). On the other hand, it is a well known property of the Vlasov equation that the dynamical evolution leads to the formation of filaments in a scale that gets smaller with time, and which leads to difficulties in its numerical integration due to the finite precision of a numerical grid [44]. For a description using individual particle dynamics, the finite computer precision also introduces a loss of information of the details of the filamentation. In

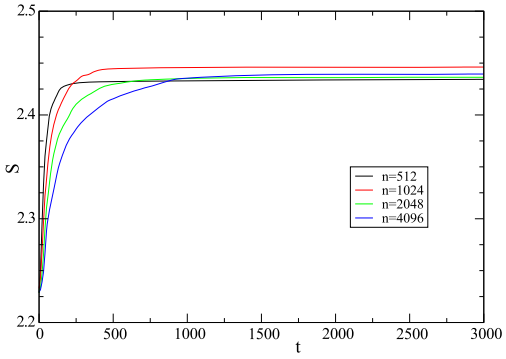

Figure 4. Entropy from the solution of the Vlasov equation as a function of time for $M_0 = 0.15$ and $e_{\text{tot}} = 0.61$ with different numerical grid resolutions $n_p \times n_\theta = n$, where n_p and n_θ are the number of points in the momentum and position directions respectively. The momentum varies in the interval $[-2.56, 2.56]$ and position from 0 to 2π.

both cases this amounts to a coarse-graining no matter the grid resolution, and results in an increase of the Gibbs entropy corresponding to $s = -f \ln f$ in equation (3) but computed using a coarse-grained distribution f_{cg}:

$$S_G = -\int \mathrm{d}\mathbf{p}\ \mathrm{d}\mathbf{r}\, f_{cg}(\mathbf{p}, \mathbf{r}; t) \ln f_{cg}(\mathbf{p}, \mathbf{r}; t), \tag{15}$$

where for simplicity and from now on we set the Boltzmann constant to unity. From now on, we will only deal with the coarse-grained one-particle distribution function and all Casimirs will be considered relative to this same distribution.

Figure 4 shows S_G for a few different grid resolutions and a waterbag initial condition. In our approach we consider indirectly the effective values of the Casimirs as given by the coarse-grained description. The size of the coarse-graining does not affect the resulting distribution function, provided it is sufficiently small, as becomes evident from figure 5 showing the Casimirs $C^{(k)}$ for a few values of k and the same initial condition. A similar behavior is observed for other choices of s. We observe that no matter the grid resolution, the final values of S_G and $C^{(k)}$ are the same, up to small numerical errors. It is beyond the scope of the present paper to discuss the effects of coarse-graining of the dynamics of the system which is discussed in greater detail in [17, 48]. The discussion above was intended to show that for the present purpose the details of the coarse-graining are not relevant in the determination of the statistical state of the system after a violent relaxation.

The values reached by the coarse-grained Casimirs, after the system has settled in a QSS, uniquely define the one-particle distribution function if we suppose that the latter depends only on the energy, as is true for one-dimensional systems from Jeans's theorem, provided some assumptions are met [10]. To show that the Casimirs determine the distribution it is sufficient to consider Casimirs of the form:

$$C^{(k)} = \int \mathrm{d}\mathbf{p}\ \mathrm{d}\mathbf{r}[f(\mathbf{p}, \mathbf{r})]^k, \tag{16}$$

with k a positive integer. Let us consider as a first approximation a distribution function with L discrete values f_i, $i = 1,\ldots, L$ such that $f(\mathbf{r}, \mathbf{p}) = f(e(\mathbf{r}, \mathbf{p})) = f_i$ in the one-particle phase space region ω_i defined by $e_{i-1} < e(\mathbf{r}, \mathbf{p}) \leqslant e_i$. By taking the limit of an infinite number of levels for f we recover a continuous function. In this way the Casimirs in equation (16) are

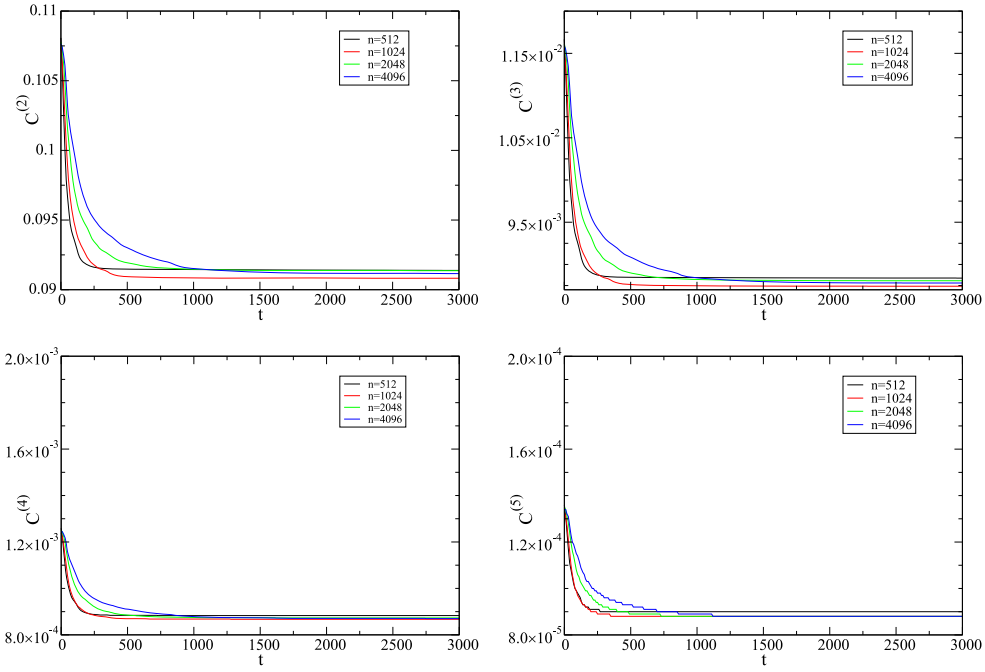

Figure 5. Casimirs $C^{(k)}$ for $k = 2, 3, 4, 5$ as defined in equation (16) as a function of time from the solution of the Vlasov equation for the same initial condition and grid resolutions as in figure 4.

rewritten as

$$C^{(k)} = \sum_{i=1}^{L} f_i^k S_i, \tag{17}$$

where S_i is the volume of the region ω_i. It is important to note that the value of $C^{(k)}$ is obtained using the coarse-grained distribution function. The values of f_i and S_i are then specified by fixing the values of a sufficient number of Casimirs.

The level curves of constant one-particle mean field energy $e(\mathbf{r}, \mathbf{p})$ are obtained from the values of S_i. This is equivalent to:

$$e(\mathbf{r}, \mathbf{p}) = \frac{p^2}{2} + \overline{V}(\mathbf{r}) = e_i,\ i = 1, \ldots, k, \tag{18}$$

with

$$\overline{V}(\mathbf{r}) = \sum_{i=1}^{k} f_i \int_{\omega_i} \mathrm{d}\mathbf{p}'\mathrm{d}\mathbf{r}' V(\mathbf{r} - \mathbf{r}') = \sum_{i=1}^{k} f_i V_i(\mathbf{r}), \tag{19}$$

and

$$V_i(\mathbf{r}) \equiv \int_{\omega_i} \mathrm{d}\mathbf{p}'\mathrm{d}\mathbf{r}' V(\mathbf{r} - \mathbf{r}'),\ S_i = \int_{\omega_i} \mathrm{d}\mathbf{p}'\mathrm{d}\mathbf{r}'. \tag{20}$$

Each value of i in equation (18) then defines the contour curves (or surfaces) of each region ω_i. This last equation defines self-consistently the boundary of each region ω_i from the set of points $(\mathbf{r}, \mathbf{p})$ satisfying it.

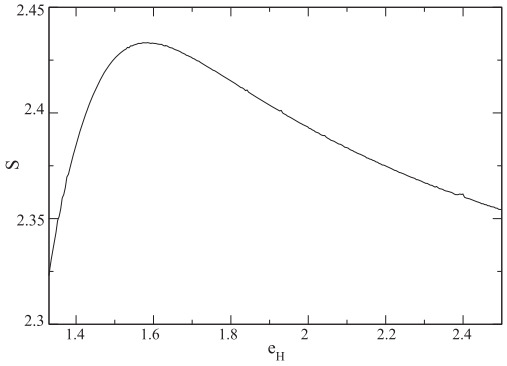

Figure 6. Gibbs entropy as a function of e_H for $M_0 = 0.15$ and $e = 0.61$. The maximum of S_B is at $e_h = 1.573$, which is very close to the value $e_H = 1.535$ obtained from the particle with maximum energy in an MD simulation.

Let us illustrate how this procedure occur swith the HMF model with a two-level distribution function ($L = 2$) as in the core-halo ansatz in equation (14), such that $e_1 = e_F$ and $e_2 = e_H$. The mean-field potential is given by equation (14), and from equation (18) we have

$$\frac{p^2}{2} = 1 - M\cos(\theta) = e_i, \tag{21}$$

with solution

$$p = \pm\sqrt{2}\sqrt{e_i - 1 + M\cos(\theta)}, \tag{22}$$

which defines the frontier curves of ω_1 and ω_2. Note that depending on the one-particle energy these curves can be composed by two disjoint curves (in the case of the HMF model), but the discussion in the previous paragraph still holds in this case. Indeed, it is straightforward to show that no two different such curves can have the same set of Casimirs of the form discussed above. The magnetization M is obtained self-consistently from equation (13).

The dynamics drives the system through a violent relaxation which then settles into a QSS. If the values of the Casimirs are known, then the distribution function can be determined. The values of the (coarse-grained) Casimirs can be directly determined from the core-halo ansatz in equation (5) as a function of the parameters η, χ, e_F and e_H, which can be determined from the value of $f = \eta$ in the initial condition, energy conservation and normalization of f. The halo energy parameter e_H still has to be determined. It is natural to expect that the system, if no dynamical constraints forbid so, evolves into the most probable state. In statistical inference, the most probable state is determined by maximizing the Gibbs entropy in equation (15) modulo any constraints. Here we only have to consider the constraints of total energy and normalization of f. The values of the Casimirs as a function of the free parameters are already given by the core-halo ansatz. Note that the Gibbs entropy is the only additive form with no statistical bias, up to a multiplicative and an additive constant, meaning that in the absence of any constraint, all states are equally probable. Any other form of the entropy than S_G leads to a bias (see for instance the discussion in [45]). At this point it is important to note that the most probable state is unique, up to some degeneracies related to conserved quantities, in the same way as the thermodynamic equilibrium is the unique state obtained as the most probable state given the total energy of the system.

In order to corroborate this statement, the Gibbs entropy as a function of the halo energy e_H for $M_0 = 0.15$ and $e = 0.61$ is shown in figure 6. The values of e_H obtained as the highest

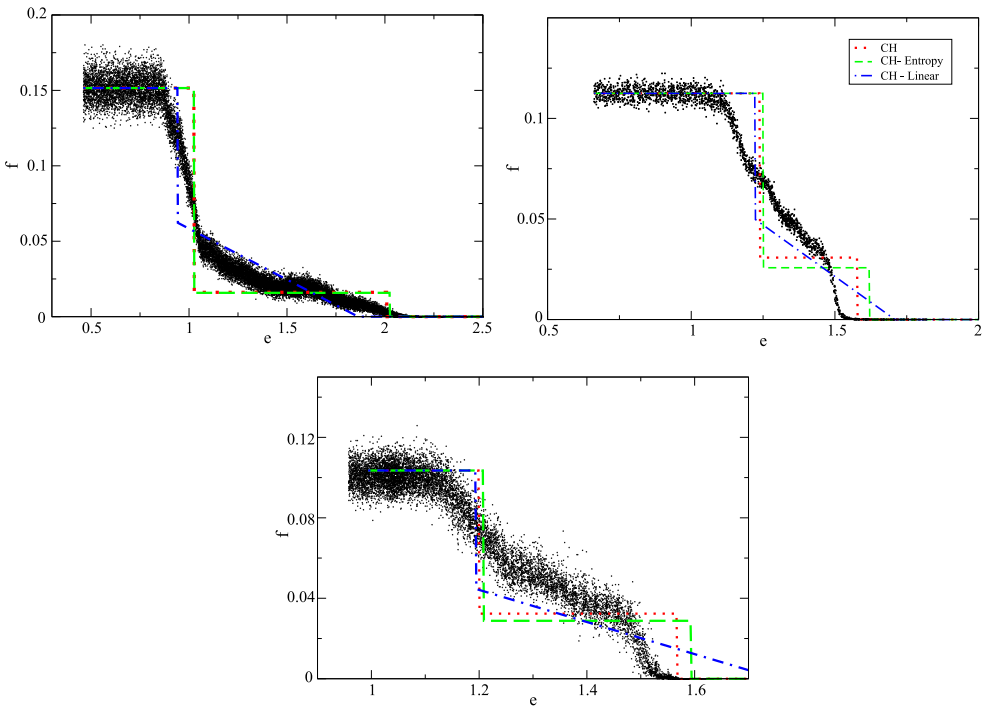

Figure 7. Distribution functions $f(e(p, \theta))$ for the HMF model as a function of single particle energy for initial magnetization $M_0 = 0.15$ and total energies per particle (a) $e_{\text{tot}} = 0.55$, (b) $e_{\text{tot}} = 0.6$, (c) $e_{\text{tot}} = 0.62$. Total simulation time is $t_f = 100\,000$ in order to allow a more complete thermalization and $N = 2\,000\,000$ (initial condition as in figure 2), except for (c) with $N = 20\,000\,000$ and $t_f = 10\,000$. The result obtained from the original core-halo approach (CH), from the present variational method (CH-Entropy) and from the modified ansatz in equation (23) (CH-Linear) are also shown.

particle energy and the maximum of S_G differ only in the second decimal digit. The non-equilibrium phase diagram for different initial magnetizations obtained from the variational approach with the ansatz in equation (5) are shown in figure 2. We observe that they are very close and even slightly better than those obtained from the original core-halo method.

A variational method opens the way to use a different ansatz as a trial function to determine the extremum of the considered functional. Here the choice of ansatz is dictated from simulation results which consistently show a core-halo structure [26]. The dependence of the distribution function $f(\theta, p)$ on the mean-field one-particle energy $e(\theta, p)$ can be obtained numerically, as shown in figure 7 for some values of the total energy per particle e_{tot} and with initial magnetization $M_0 = 0.15$. The core-halo distribution function as obtained from both the original and the variational method (i.e. with e_H determined from entropy maximization) are also shown. Although the separation in a core and a halo becomes less evident as the energy augments, both yield very similar results. From figure 7 it is quite natural to try a different ansatz given by:

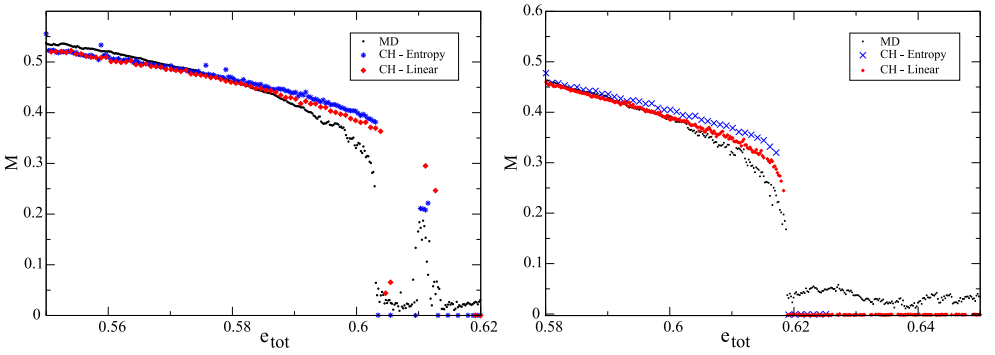

Figure 8. Final magnetization after the violent relaxation as a function of energy for the original core-halo (CH-Entropy) and the modified ansatz in equation (23) (CH-Linear), where in both cases e_H was determined from the entropy maximum. Initial magnetizations are: (a) $M_0 = 0.15$, (b) $M_0 = 0.3$. The values obtained from the distribution function in equation (5) are also plotted for comparison. Both cases were obtained maximizing the entropy.

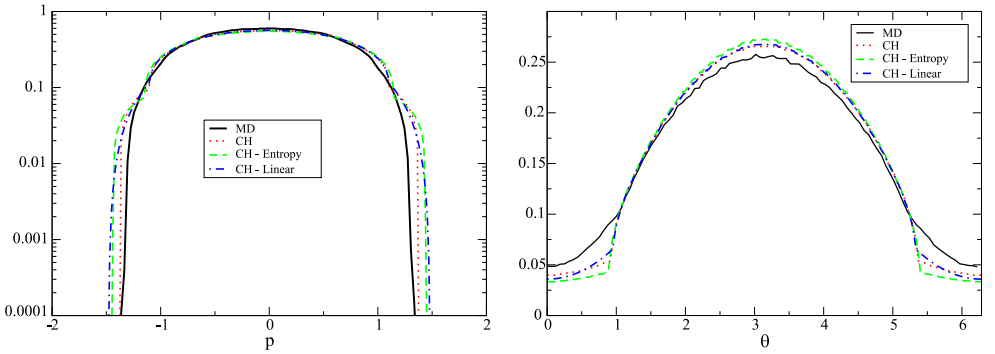

Figure 9. Left panel: mono-Log plot of the velocity distribution function from MD, CH, CH-Entropy, and CH-Linear for $M_0 = 0.15$ and $e = 0.6$. Right panel: the spatial distribution function for the same cases.

$$f(\mathbf{r}, \mathbf{p}, t_v) = \eta\, \Theta(e_F - e(\mathbf{r}, \mathbf{p})) + \chi \Theta(e(\mathbf{r}, \mathbf{p}) - e_F) \times \Theta(e_H - e(\mathbf{r}, \mathbf{p}))\left[1 - \frac{e(\mathbf{r}, \mathbf{p}) - e_F}{e_H - e_F}\right], \tag{23}$$

which is essentially a core with constant f-value η, also given by the value of the initial waterbag distribution, but with a linearly decreasing halo starting at the f-value χ. The resulting values of magnetization as a function of e after the violent relaxation are shown in figure 8 with a little improvement for some energy intervals. The ansatz in equation (23) is closer to the dependence of the distribution functions in the one-particle energy e as obtained from MD simulations, at least for the cases considered here, as can be seen in figure 7. The velocity and position distribution functions for the different approaches considered here are given in figure 9, with little differences from one another. The Fermi and halo energies for the case $M_0 = 0.15$ are shown in figure 10, with substantial differences. We note that in our results the value of e_F and consequently also that of e_H are bigger than the average total energy per particle, indicating that the majority of particle are concentrated on the core of the

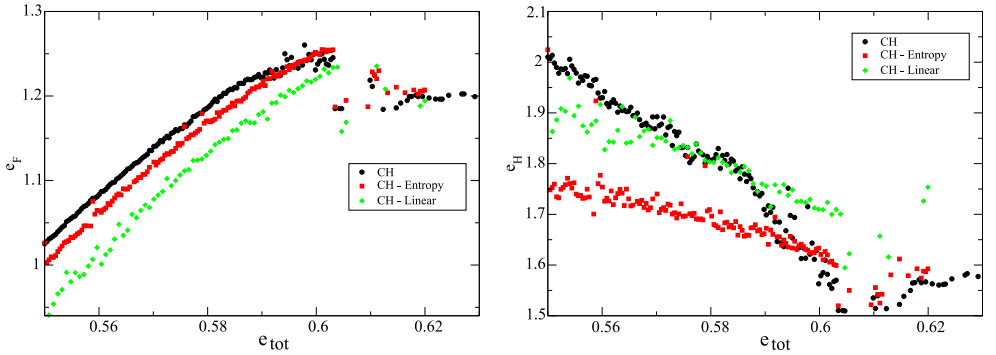

Figure 10. Fermi energy e_F and halo energy e_H for $M_0 = 0.15$ as a function of total energy per particle for CH, CH-Entropy and CH-Linear.

distribution. Our results also show that relevant physical observables have little sensitivity in the details of the halo part of the distribution.

The (non-equilibrium) entropy for the usual core-halo distribution in equation (5) is shown in figure 11 as a function of energy e and e_h for $M_0 = 0.15$. The discontinuous phase transition is related to a discontinuity in the entropy at the critical energy and, quite interestingly, the entropy decreases in the phase transition, as energy increases, which would be impossible for an equilibrium phase transition. This means that at the onset of the parametric resonance that triggers the halo formation and the phase transition, the region in the (θ, p) single particle phase space of states accessible to the system and compatible with all constraints (energy and Casimir invariants) in fact shrinks at the phase transition, while the energy increases. By comparing figures 3 and 11 we note the complicated phase reentrance structure observed in the latter is also associated with discontinuities in the non-equilibrium Gibbs entropy resulting from the core-halo ansatz.

Although all expressions used here are analytic in the free parameters χ, e_F, e_H and M, the resulting non-equilibrium entropy has discontinuities at some values of the single particle energy e. This is due to the fact that χ, e_H and the magnetization M are obtained from the solution of highly nonlinear equations. The solutions of the latter can present discontinuities when a given parameter changes, as the total energy e or the initial magnetiztion M_0.

The interplay between Gibbs statistics and dynamical regimes has already been studied previously by many authors in both short- and long-range interacting systems [49–52]. Here we have shown evidence of a similar interplay between a dynamic property (parametric resonance) and a quasi-stationary non-equilibrium statistical distribution.

4. Concluding remarks

We have shown that the core-halo approach of Levin and collaborators can be recast as a variational principle when the Gibbs entropy maximization principle is considered alongside the energy and mass conservation (normalization of f), with the final magnetization obtained self-consistently. The information on the Casimir values is in fact embedded in the ansatz for the core-halo distribution and maximizing the entropy is then equivalent to stating that the system evolves towards the most probable state given the energy, initial magnetization and the information on the final values of the coarse-grained Casimirs in the core-halo ansatz. The results obtained using the present variational approach are compatible with those obtained

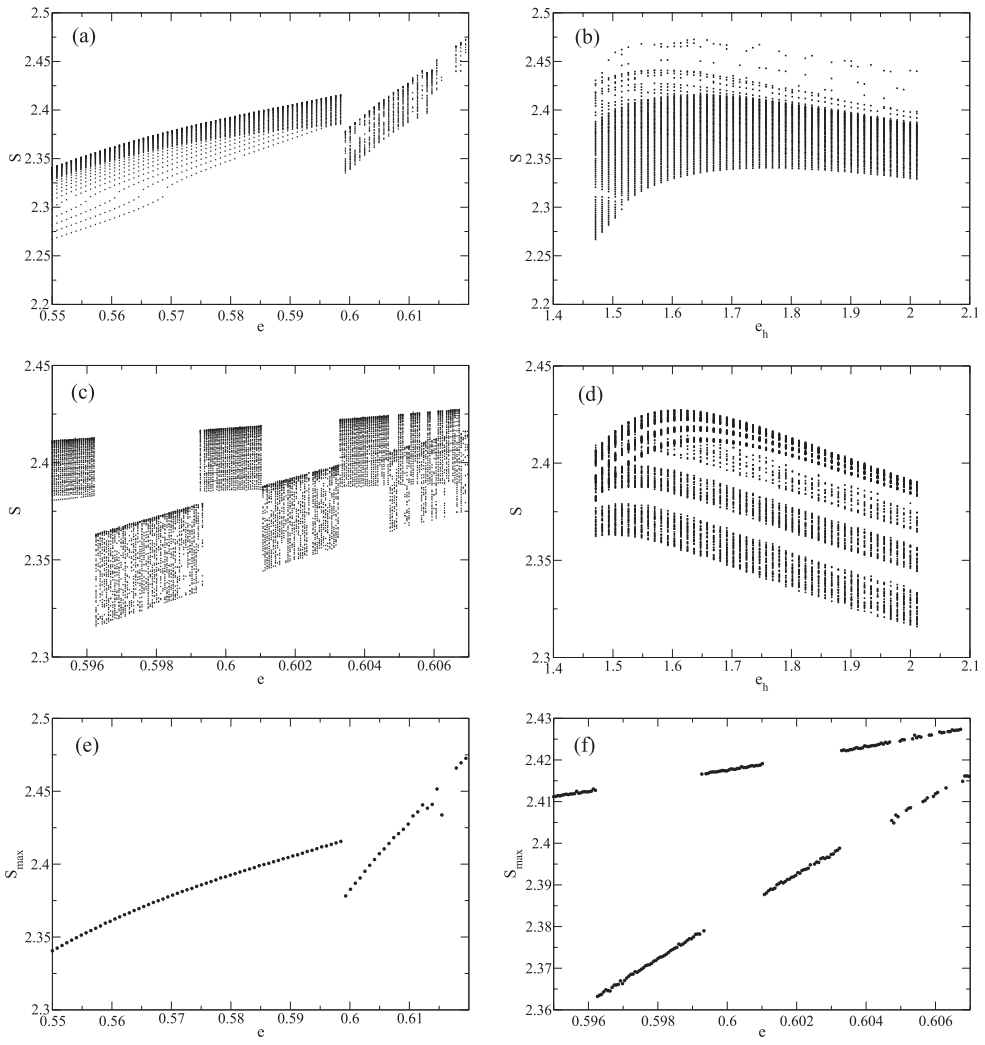

Figure 11. (a) Gibbs entropy in equation (15) for the core-halo distribution in equation (5) as a function of total energy per particle e for different values of the halo energy e_h in the interval $1.46 < e_h < 2.0$ and initial magnetization $M_0 = 0.15$. (b) Entropy as a function of the core-halo energy e_h for the interval of energy values e in (a). (c) Same as (a) but zooming around the energy value of the phase transition. (d) Same as (b) but with an interval for e around the phase transition. (e) Maximum Gibbs entropy $S_{\max}$ as a function of e. (f) Same as (e) but zooming on the energy value of the phase transition. Note that phase reentrances also correspond to discontinuities of the entropy.

previously for the HMF model, and slightly better for some values of energy and initial magnetization. We also obtained, for the first time using a theoretical approach, the phase reentrances of the HMF model, and showed that they also result from discontinuities of the entropy that result straightforwardly from the information contained in the core-halo distribution. It is quite interesting that in the non-equilibrium case the phase transition is not always due to a discontinuity on a derivative of the entropy, but of the entropy itself.

We have also shown that other forms for the distribution function as a function of the one-particle energy can be used with similar results, provided the number of parameters is the same. This is in fact a common advantage of variational methods, allowing the use of different trial functions in the functional to maximize. Our approach greatly simplifies the application of the core-halo approach as no envelope equation is required to determine the halo energy. Although the present approach works well with HMF systems and is robust if one admits that the system must evolve towards the most probable states given a set of constraints, it must still be applied to other long-range interacting systems in order to assess its general validity, which is the subject of ongoing work.

Another important result of the present paper concerns the link between an out-of-equilibrium dynamical phenomenon, the parametric resonance causing the non-equilibrium phase transition, and the entropy as a statistical property of a (non-equilibrium) stationary state. The dynamics leads the system into its final state (in the Vlasov limit $N \to \infty$) and, in some still undetermined way, must have a signature in the entropy maximum corresponding to this state. Although the core-halo approach is not a complete theory for the determination of the outcome of the violent relaxation evolution, the present work shows the relevance of statistical concepts such as entropy maximization subject to dynamical constraints in the form of Casimir and energy conservation.

Acknowledgments

The author acknowledges partial financial support by CAPES and CNPq (Brazilian Government agency).

References

[1] Campa A, Dauxois T, Fanelli D and Ruffo S 2014 *Physics of Long-Range Interacting Systems* (Oxford: Oxford Univ. Press)
[2] Campa A, Dauxois T and Ruffo S 2009 *Phys. Rep.* **480** 57
[3] Filho T M R, Amato M A, Santana A E, Figueiredo A and Steiner J R 2014 *Phys. Rev.* E **89** 032116
[4] Koyama H, Konishi T and Ruffo S 2008 *Commun. Nonlinear Sci. Numer. Simul.* **13** 868
[5] Dauxois T, Ruffo S, Arimondo E and Wilkens M (ed) 2002 *Dynamics and Thermodynamics of Systems with Long-Range Interactions* (Berlin: Springer)
[6] 2008 Dynamics and thermodynamics of systems with long-range interactions: theory and experiments *AIP Conf. Proceedings* vol 970
[7] Dauxois T, Ruffo S and Cugliandolo L F (ed) 2010 *Long-Range Interacting Systems, Les Houches 2008, Session XC* (Oxford: Oxford Univ. Press)
[8] Lynden-Bell D 1967 *Mon. Not. R. Astr. Soc.* **136** 101
[9] Braun W and Hepp K 1977 *Commun. Math. Phys.* **56** 125
[10] Binney J and Tremaine S 2009 *Galactic Dynamics* II ed. (Princeton: Princeton University Press)
[11] Bindoni D and Secco L 2008 *New Astr. Rev.* **52** 1
[12] Shu F H 1978 *ApJ* **225** 83
[13] Kull A, Treumann R A and Böhringer H 1997 *ApJ* **484** 58
[14] Nakamura T K 2000 *ApJ* **531** 739
[15] Arad I and Lynden-Bell D 2005 *Mon. Not. R. Atron. Soc.* **361** 385
[16] Arad I and Johansson P H 2005 *Mon. Not. R. Atron. Soc.* **362** 252
[17] Firpo M-C, Doveil F, Elskens Y, Bertrand P, Poleni M and Guyomarc'h D 2001 *Phys. Rev.* E **64** 026407
[18] Firpo M-C and Doveil F 2002 *Phys. Rev.* E **65** 016411
[19] da F P, Benetti C, Teles T N, Pakter R and Levin Y 2012 *Phys. Rev. Lett.* **108** 140601
[20] Levin Y, Pakter R and Teles T 2008 *Phy. Rev. Lett.* **100** 040605

[21] Teles T, Pakter R and Levin Y 2009 *App. Phys. Lett.* **95** 173501
[22] Pakter R and Levin Y 2011 *Phys. Rev. Lett.* **106** 200603
[23] Levin Y, Pakter R and Rizzato F 2008 *Phys. Rev.* E **78** 021130
[24] Teles T N, Levin Y, Pakter R and Rizzato F B 2010 *J. Stat. Mech.* **2010** P05007
[25] Teles T, Levin Y and Pakter R 2011 *Mon. Not. R. Astron. Soc.* **417** L21
[26] Levin Y, Pakter R, Rizzato F B, Teles T N and Benetti F P C 2014 *Phys. Rep.* **535** 1
[27] Antoniazzi A, Elskens Y, Fanelli D and Ruffo S 2006 *Eur. Phys. J.* B **50** 603
[28] Barré J, Dauxois T, De Ninno G, Fanelli D and Ruffo S 2004 *Phys. Rev.* E **69** 045501 (R)
[29] Antoniazzi A, Fanelli D, Barré J, Chavanis P H, Dauxois T and Ruffo S 2007 *Phys. Rev.* E **75** 011112
[30] Yamaguchi Y Y, Barré J, Bouchet F, Dauxois T and Ruffo S 2004 *Physica* A **337** 36
[31] Campa A, Giansanti A and Morelli G 2007 *Phys. Rev.* E **76** 041117
[32] Campa A, Chavanis P H, Giansanti A and Morelli G 2008 *Phys. Rev.* E **78** 040102 (R)
[33] Jain K, Bouchet F and Mukamel D 2007 *J. Stat. Mech.* P11008
[34] de Buyl P arXiv:1210.6316
[35] Antoni M and Ruffo S 1995 *Phys. Rev.* E **52** 2361
[36] de Buyl P, Fanelli D and Ruffo S 2012 *Centr. Eur. J. Phys.* **10** 652
[37] Staniscia F, Chavanis P H and Ninno G De 2011 *Phys. Rev.* E **83** 051111
[38] Staniscia F, Chavanis P H, De Ninno G and Fanelli D 2009 *Phys. Rev.* E **80** 021138
[39] Antoniazzi A, Fanelli D, Ruffo S and Yamaguchi Y Y 2007 *Phys. Rev. Lett.* **99** 040601
[40] Ogawa S and Yamaguchi Y Y 2011 *Phys. Rev.* E **84** 0611450
[41] Yoshida H 1990 *Phys. Lett.* A **150** 262
[42] Filho T M R 2014 *Comp. Phys. Comm.* **185** 1364
[43] Filho T M R, Amato M A and Figueiredo A 2012 *Phys. Rev.* E **85** 062103
[44] Filho T M R 2013 *Comp. Phys. Comm.* **184** 32
[45] Figueiredo A, Amato M A and Filho T M R 2006 *Physica* A **367** 191
[46] Filho T M R, Santana A E, Amato M A and Figueiredo A 2014 *Phys. Rev.* E **90** 032133
[47] Filho T M R, Figueiredo A and Amato M A 2005 *Phys. Rev. Lett.* **95** 190601
[48] Doveil F, Firpo M-C, Elskens Y, Guyomarch D, Poleni M and Bertrand P 2001 *Phys. Lett.* **284** 279
[49] Escande D, Kantz H, Livi R and Ruffo S 1994 *J. Stat. Phys.* **76** 605
[50] Tamarit F and Anteneodo C 2000 *Phys. Rev. Lett.* **84** 208
[51] Baldovin F, Moyano L G and Tsallis C 2006 *Eur. Phys. J.* B **52** 113
[52] Yang H-l and Radons G 2008 *Phys. Rev.* E **77** 016203